One method for HJ-1-A HSI and CCD data fusion

Wencheng Xiong [1, 2], Yun Shao [1], Wenming Shen [2], Rulin Xiao [2], Zhuo Fu [2]and Yuanli Shi [2]

1. Institute of Remote Sensing Application, Chinese Academy of Sciences, Beijing China;
2. Satellite Environment Application Center, Ministry of Environment Protection, Beijing, China.

E-mail:wencheng11@sina.com

Abstract. HJ-1-A satellite, developed by China independently, was equipped with two sensors of Hyper Spectral Imager (HSI) and multispectral sensor (CCD). In this paper, we examine the benefits of combining data from CCD data (high-spatial-resolution, low-spectral-resolution image) with HSI data (low -spatial-resolution, high -spectral-resolution image). Due to the same imaging time and similar spectral regime, the CCD and HSI data can be registered with each other well, and the difference between CCD and HSI data mainly is systematic bias. The approach we have been investigating compares the spectral information present in the multispectral image to the spectral content in the hyperspectral image, and derives a set of equations to approximately acquire the systematic bias between the two sensors. The systematic bias is then applied to the interpolated high-spectral CCD image to produce a fused product. This fused image has the spectral resolution of the hyperspectral image (HSI) and the spatial resolution of the multispectral image (CCD). It is capable of full exploitation as a hyperspectral image. We evaluate this technique using the data of Honghe wetland and show both good spectral and visual fidelity. An analysis of SAM classification test case shows good result when compared to original image. All in all, the approach we developed here provides a means for fusing data from HJ-1-A satellite to produce a spatial-resolution-enhanced hyperspectral data cube that can be further analyzed by spectral classification and detection algorithms.

1. Introduction

HJ-1-A satellite was launched successfully September 6, 2008, which were developed by china independently. Up to now, a large number of images have been downloaded from the satellites. Therefore, how to remove redundancy and fuse these data is an important research direction. In addition, Hyperspectral imaging systems are receiving increasing attention for a wide variety of military, intelligence, civil and commercial systems. The reason is that a hyperspectral imager provides information on scene content that is not obtainable from single-band or multispectral sensors. In this paper, we examined the benefits of combining data from CCD data (high-spatial-resolution, low-spectral-resolution image) with HSI data (low-spatial-resolution, high -spectral-resolution image).

The deployment of a high-spatial-resolution space-based hyperspectral imaging sensor presents many technological challenges. For an optical imager system, image spatial resolution and spectral resolution is a contradiction. A high spectral resolution imager cannot have high spatial resolution at a given S/N ratio (signal to noise ratio). The spatial resolution of the current hyperspectral imager,

especially the imagers on satellite platform, is not very high, such as the Hyperion sensor onboard the NASA EO-1 spacecraft with a spatial resolution of 30 meters [1].

China has only one hyperspectral sensor in Earth orbit, the HSI sensor onboard the HJ-1-A satellite. The HJ-1-A satellite was equipped with a CCD imager which has 30-meter spatial resolution and four bands, and a hyperspectral imager which has 100-meter spatial resolution and 115 bands (specific parameters is in Table 1).

Table 1. HJ-1-A Satellite Parameters Table

Platform	Sensor	Band	Wavelength	Resolution	Swath
HJ-1A	CCD	B01	0.43-0.52 μm	30 m	360 km
		B02	0.52-0.60 μm		
		B03	0.63-0.69 μm		
		B04	0.76-0.9 μm		
	Hyperspectral Imager（HSI）		0.45-0.95 μm （115bands）	100 m	50 km

Typically, the spectral imagery data from high-spatial-resolution, low-spectral-resolution sensor and the high-spectral resolution, low-spatial-resolution sensor are treated separately. The hyperspectral imagery is a rich source of information that lends itself to both physical processing techniques, such as the linear-mixture-model-based techniques, and the Reed-Xiaoli (RX) anomaly detection algorithm. Therefore, how to fuse the HSI data with CCD data and produce a new high-spatial and high-spectral image is important.

In general, image fusion methods mainly include image fusion based on color space, image fusion based on mathematics / statistics, image fusion based on multi-resolution analysis and intelligent image fusion. The color space fusion can be RGB synthetics, IHS transformation, or Brovey transformation. Image fusion based on mathematics and statistics can be ratio fusion, addition multiplication fusion, PCA (Principal Component Analysis) method, HPF (High Pass Filter) method, Bayesian estimation fusion, EM (Expectation Maximum) fusion, or image fusion based on non-negative matrix factorization. Image fusion based on multi-resolution analysis can be pyramid transformation, wavelet transformation, neural network fusion, or fuzzy theory fusion. In fact, the fusion methods could be used comprehensively to reach the application target [2].

However, these methods above considered less about the spectrum characteristics and the waveform changes of the fused hyperspectral images. To reduce the waveform distortion of fused image, a model of spatial fusion based spectral reversion (SFSR) and a fusion method based on spectral decomposition were proposed for the high-spectral and panchromatic data [3-4]. These methods not only improved the image spatial resolution, but also maintained the waveform of the original high spectral data as much as possible. For multi-spectral and high-spectral images fusion, CRISP model was developed [5]. These methods were designed for common images without giving any consideration about characteristics of HJ-1-A satellite. In this paper, we took full advantage of the characteristics of HJ-1-A satellite, such as the same imaging time and similar spectral regime, to minimize the spectral distortion when HSI and CCD data were fused.

2. Approach

The CCD and HSI images of Honghe National Nature Reserve wetland were chose for this study. The HSI and CCD data sets were taken from the same fixed platform, so there were little registration errors and changes in scene content. The two images were calibrated using flat field calibration method, and then were analyzed to find out the features of the two data sets. Based on these features, the fusion method was developed.

2.1. Flat Field Calibration

Before the fusion of CCD and HSI of HJ-1-A satellite, Sensor calibration and atmospheric correction should be applied for the two images to acquire the ground surface reflectivity. For the lack of the atmospheric parameters, the flat field calibration, one of spectral inversion statistical models, was used.

First, one large region with high brightness and flat spectral response curve was chose as the flat field. Then the average spectrum of the flat field was used as the solar spectrum at the satellite passing time. The DN (digital number) value of each pixel was divided by the average radiation spectrum and became the surface relative reflectivity. The atmospheric influence was eliminated from the two images.

$$\rho_\lambda = R_\lambda / F_\lambda$$

ρ_λ is relative reflectivity; R_λ is radiance value of single pixel; F_λ is average radiation spectrum of the flat field.

Atmospheric correction using flat field calibration method has two important prerequisites: 1) there are no visible absorption spectrum characteristics in the average reflectance spectrum of the flat field; 2) the flat field spectrum should be similar to the solar spectrum. According to the features of the study area, the flat field selected in this study was shown in Figure 1.

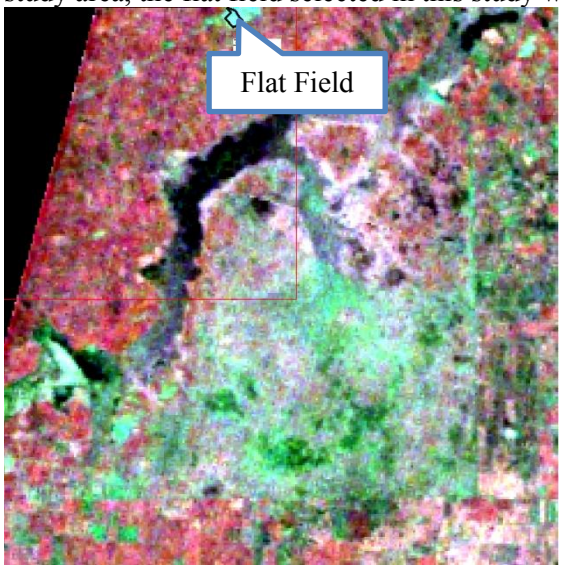

Figure1. Flat Field of the Honghe Wetland for Calibration

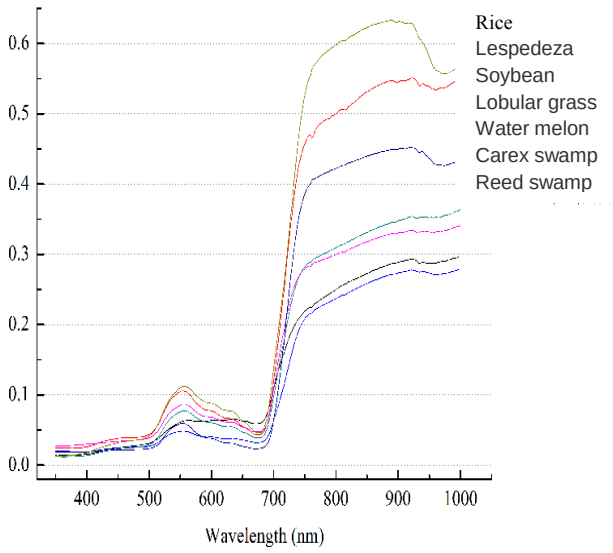

Figure 2. Spectra of typical surface objects（the annotations are ordered by values at 900nm）

2.2. Spectra Analysis

We chose typical objects from the calibrated images, and analyzed the spectra of these objects on HSI and CCD images. From Figure 2 and 3, we can see: 1) a higher reflectivity and obvious near-infrared reflectance peak presents in the forest spectrum, this matches the ground spectrometer measurements. The other typical object spectra also show a good match between image spectra and the ground spectrometer measurements spectra. 2) There are similar shapes between the spectral curves of typical objects in CCD and HSI images. 3) The relative reflectivity of HSI is generally higher than that of CCD because HSI has greater radiometric resolution. (Radiometric resolution refers to the number of distinguished gray ladder, format of HSI image is an unsigned integer, and CCD is Byte). 4) The spectral curves of typical objects in HSI image are more sophisticated than these in CCD image due to the higher spectral resolution.

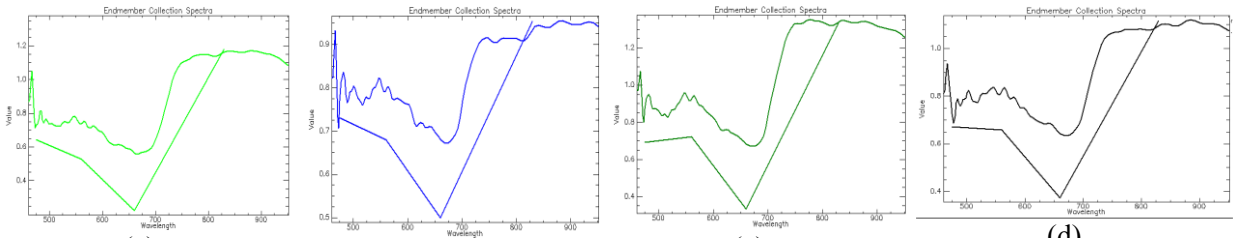

(a) (b) (c) (d)

Figure 3. Typical objects Image Spectra (the top is HSI, the bottom is CCD), (a) - Forest Image Spectra, (b)- Marsh Image Spectra, (c)- Bush Image Spectra, (d)- Grass Image Spectra

2.3. Fusion Algorithm

CCD and HSI calibrated images of HJ-1-A satellite are co-registered well, for the same imaging time. However, there is systematic bias for the two optical imagers, due to the different central wavelength and different imaging signal response of CCD and HSI. The fusion algorithm is designed to eliminate systematic bias between the two optical systems, based on the simultaneity of the two systems. The images of CCD and HSI were interpolated and fused at spectral domain. The algorithm can be described as:

a) The original CCD data (CCD_{30}) was interpolated to 100m as the resolution of HSI, we got CCD_{100}; then, the four bands of CCD_{100} were interpolated to 115bands according to wavelength, we got $CCD_{100-115}$.

$$CCD_{100} = congrid(CCD_{30})$$

$$CCD_{100-115} = interpol(CCD_{100}, 4, 115)$$

Congrid refers to interpolation at 2-dimension; Interpol refers to interpolation at one dimension.

b) CCD and HSI Images have the different spectrum dynamic range, so HSI image was normalized based on CCD image, we got normalized HSI data HSI_{NM};

$$Mult = \{Max(CCD_{100-115}[m,n,*]) - Min(CCD_{100-115}[m,n,*])\} / \{Max(HSI[m,n,*]) - Min(HSI[m,n,*])\}$$

$$HSI_{NM}[m,n,*] = (HSI[m,n,*] - Min(HSI[m,n,*])) * Mult + Min(CCD_{100-115}[m,n,*])$$

$Mult$ is ratio of dynamic ranges of CCD and HSI, $CCD_{100-115}[m,n,*]$ refers to all values of the m-th column, n-th row of the $CCD_{100-115}$ matrix. The others have the same meaning.

c) $CCD_{100-115}$ was subtracted by HSI_{NM}, we could get systematic bias $Delta_{100-115}$

$$Delta_{100-115} = HSI_{NM} - CCD_{100-115}$$

d) The 4-band CCD was interpolated to 115 bands, we got CCD_{30-115}; Systematic bias ($Delta_{100-115}$) was resampled to 30m, we got $Delta_{30-115}$.

$$CCD_{30-115} = interpol(CCD_{30}, 4, 115)$$

$$Delta_{30-115} = congrid(Delta_{100-115})$$

e) CCD_{30-115} added the systematic bias of two optical systems ($Delta_{30-115}$), we can get the fusion image (CCD_HSI).

$$CCD\_HSI = CCD_{30-115} + Delta_{30-115}$$

3. Results

3.1. Visual Evaluation

Image fidelity is good. From the aspect of the visual effect of RGB three-band composite, the fused image is approximate to the original CCD image at spatial resolution and color representation, and shows better representation than the original HSI image. There are clearer texture details, especially boundaries of different vegetation and more vivid color in fused image, due to the greater spectral dynamic range and higher spatial resolution.

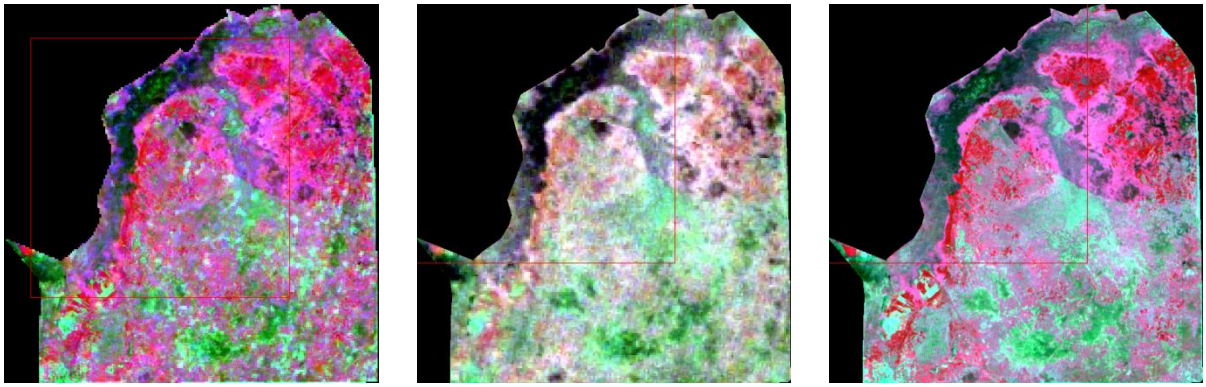

Fused Result Image | Original HSI (R-100，G-70，B-40) | Original CCD（R-4，G-3，B-2）

Figure 4. Comparison between fused image and original images

3.2. Spectra comparison

Four typical object spectra from the fused image and HSI image were selected respectively for comparison: forest spectra, grass spectra, bush spectra and marsh spectra. These spectra are shown in Figure 5, the black line being the fused image spectrum and the red line being the original HSI image spectrum. From Figure 5, we could see that the peaks and valleys of both waveforms are basically same, although the spectral dynamic range of fused image is greater than that of the original.

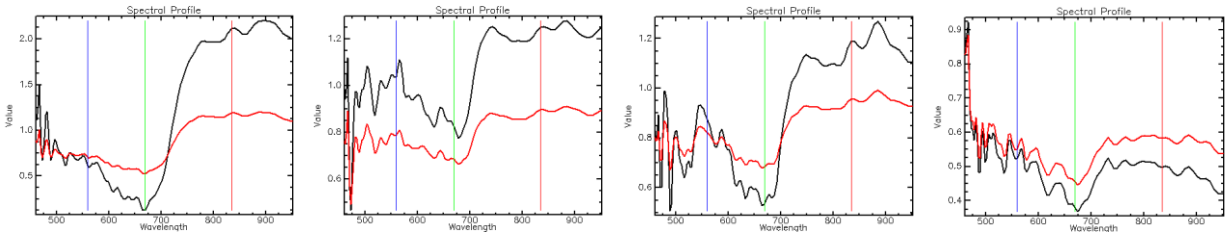

Forest Spectra | Grass Spectra | Bush Spectra | Marsh Spectra

Figure 5. Comparison between fused image and HSI (red-HSI, black-fused image)

3.3. Evaluation for classification

The HSI image and fused image were classified with SAM (Spectrum Angle Mapping). Figure 6 and 7 show that map-spot of HSI classification map is greater, and the map-spot of fused image classification map is finer. This can be ascribed to the fused image's finer representation for surface objects at spatial domain.

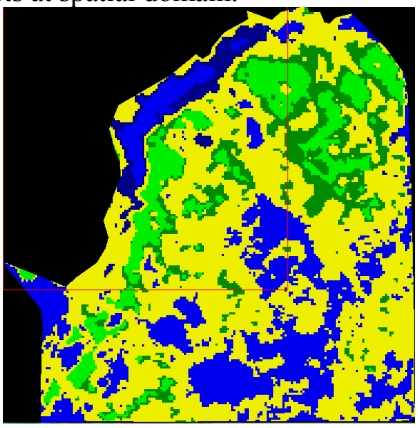

Figure 6. HSI SAM classification result for original

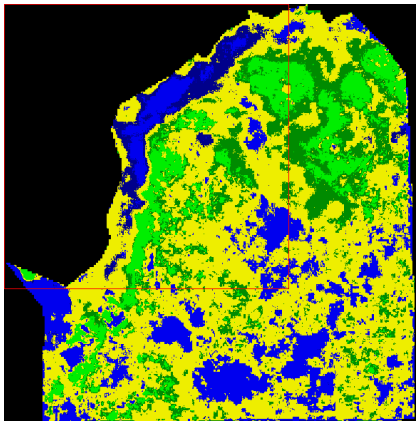

Figure7. SAM classification result for fused data

4. Discussion and Conclusions

Detection algorithms generally perform best when the sensor's instantaneous field of view is comparable to or smaller than the size of the anomalies. Consequently, it is important to investigate techniques which can fuse high-spatial-resolution information with data from a low-spatial-resolution hyperspectral imaging sensor.

The approach discussed herein was designed for HJ-1-A satellite. The approach we have developed provides a method to generate high-spatial-resolution spectral imagery by combining multispectral CCD data with data from hyperspectral HSI data having high spectral resolution but low spatial resolution.

The algorithm is unique in several ways. It includes the ability to improve the spatial resolution of HSI data by using higher-spatial-resolution CCD imagery from the same satellite platform. It uses a novel mathematical approach to combine HSI and CCD data to produce a fused image that has high spectral fidelity. We applied this approach to a set of Honghe wetland images from HJ-1-A satellite, and the fused image showed a good result compared to the original data. All in all, this approach provides a means for fusing data from HJ-1-A satellite to produce a spatial-resolution-enhanced hyperspectral image that can be further analyzed by spectral classification and detection algorithms.

Acknowledgements

This research was Funded by Key Laboratory of Geo-Informatics of National Administration of Surveying, Mapping and Geoinformation of China (NO.201126) and a grant from Special Environment Scientific Research Fund for Public Welfare (No.201109043).

References

[1] Ungar S G, Jay S P, Jeffrey A.M and Dennis R 2003 Overview of the Earth Observing One (EO-1) Mission *IEEE Trans. Geosci.and Remote Sensing.* **41** 1149-1159

[2] Zhao Y S 2003 Principles and Methods of Analysis of Remote Sensing Applications *Beijing: China Science Press*

[3] Tong Q X, Zhang B, Zheng L F 2006 Hyperspectral Remote Sensing *Beijing: Higher Education Press*

[4] Gary D R., Harry N G, Schott J R 2000 Evaluation of Two Applications of Spectral Mixing Models to Mmage Fusion *Remote Sensing of Environment*. **71** 272-281

[5] Michael E W, Scott G B, Anthony J. R 2007 Hyperspectral Image Sharpening Using Multispectral Data *IEEE Aerospace Conference.*

[6] Harry N G, John R S 1998 Application of Spectral Mixture Analysis and Image Fusion Techniques for Image Sharping *Remote Sensing of Environment*. **63** 85-94

[7] Dong G J, Zhang Y S, Fan Y H 2006 Image Fusion for Hyperspectral Data of PHI and High-resolution Aerial Image *J. Infrared Millim Waves*. **25** 123~126.

[8] Ranchin T and Lucien W 2000 Fusion of High-Spatial- and Spectral-Resolution Images The ARSIS Concept and Its Implementation *Photogrammetric Engineering and Remote Sensing* **66** 49-56